$StressLife_{tc}$ – NDT-related assessment of the fatigue life of metallic materials

Peter Starke, Kaiserslautern, Germany

Weight-optimized component design as well as a reliable estimation of the lifetime of metallic materials and components requires a comprehensive understanding of fatigue processes and a systematic investigation of the underlying fatigue behavior. Therefore, nondestructive testing methods, digitalization of measurement techniques as well as signal processing can be combined with a short-term procedure in order to acquire potentially more information about fatigue processes, while experimental effort and costs are reduced significantly. This leads not only to considerable advantages over conventional methods for determining S-N curves, but also over established short-term procedures, due to the possibility of applying this information from just a few specimens to attain fatigue life calculations. The $StressLife_{tc}$ approach is a new short-term calculation method which considers the nonlinear relation between the elastic, elastic-plastic and plastic portion of the material response in the deformation process. Within the scope of the present work, the change in temperature of SAE 1045 (C45E) specimens was measured during fatigue tests via an infrared camera in order to feed the thermal response back into the new $StressLife_{tc}$ approach for a reliable fatigue life calculation.

Article Information

Correspondence Address
Prof. Dr.-Ing. Peter Starke
Department of Materials Science and Materials Testing
University of Applied Sciences Kaiserslautern
Schoenstr. 11
D-67659 Kaiserslautern, Germany
E-mail: peter.starke@hs-kl.de

Keywords
Thermography, Magnetics, Non-Destructive Testing, Fatigue Life Evaluation, Metallic Materials

Besides appropriate dimensioning and choice of materials, understanding fatigue behavior is fundamental for the reliable and economical operation of fatigue-loaded components. This understanding is very closely linked to microstructure and characterized by complex interrelated processes. The first systematic fatigue investigations were performed around 150 years ago by August Wöhler, who was one of the pioneers in this field. The S-N curve, which is still used today for an optimized material selection and an enhanced component design, is also often called the "Wöhler-curve" and provides the relationship between an applied load and the lifetime of a specimen [1-3].

Cyclic loading on metallic materials causes micro-plastic deformations and, due to cyclic softening and/or hardening processes, leads to the formation of characteristic dislocation structures and deformation properties that may be the initial point of fatigue cracks. Fatigue-induced property changes can lead to the formation and propagation of cracks and ultimately to failure. Changes in mechanical material behavior during cyclic loading are usually characterized by evaluating the plastic strain amplitude [1, 2], which can be expressed as a function of the number of cycles N in so-called cyclic deformation curves. In the fatigue experiments described below, change in temperature [3, 4] and change in magnetic properties [5-6] were determined with high precision. In general, the changes in these physical quantities are directly linked by cross-effects to microstructural changes in the bulk material obtained during quasi-static or even fatigue loading.

Generating S-N data for the design process of structures and components as well as for an optimal material selection needs to be performed in a quick and cost-effective way. Even today, there is still an intense discussion with respect to the validity of the Palmgren-Miner linear damage accumulation rule and the importance of non-linearity in a damage accumulation process [7]. The understanding of the load-damage-relation is of major importance for the development of fatigue life calculation methods or evaluation models, which are aimed at predicting the lifetime of a specimen, a component or even a whole structure starting at the initial state or in any state during service.

Up till now, several short-term fatigue life calculation methods have been available, one of them is the physically based fatigue life calculation method PhyBaL [8]. PhyBaL was developed at the Institute of Materials Science and Engineering at the University of Kaiserslautern and is a procedure by which the complete stress-strain as well as S-N curve of a material is generated by three experiments on un-notched specimens, reducing the amount for experimen-

tation by an order of magnitude when compared to conventional approaches.

Within the fatigue life calculation method StressLife$_{tc}$ (tc = trend curve calculation), based on principles similar to PhyBaL, fatigue data from one load increase and two constant amplitude tests are used to evaluate the fatigue strength as well as the fatigue limit of a metallic material [9].

This short-term procedure results in an enormous reduction in experimental time and cost and offers the possibility of investigating even more fatigue relevant parameters like mean stress, residual stress, material conditions, elevated temperatures etc. with the same number of specimens, in comparison with the conventional way to generate a simple S-N curve. Consequently, safety factors can be defined more individually, and replacement strategies benefit from flexible characteristics.

StressLife$_{tc}$ combines the potential of NDT-methods, the digitalization of measurement techniques as well as signal processing to acquire comprehensive information concerning fatigue behavior in tandem with a simultaneous reduction of experimental efforts and cost, which ultimately means fewer experiments but more information.

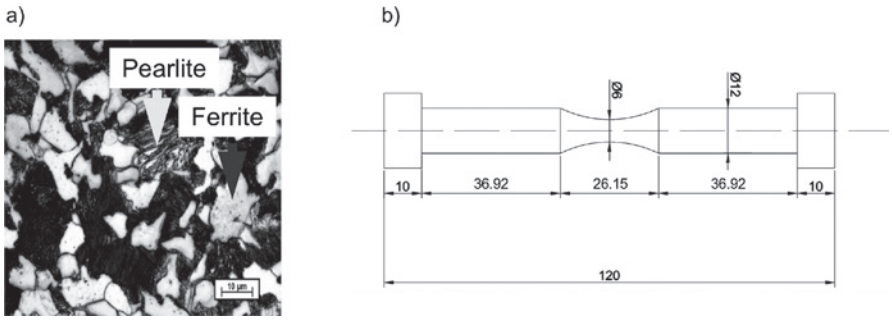

Figure 1: a) Pearlitic-ferritic microstructure of normalized SAE 1045 (C45E) and b) specimen geometry

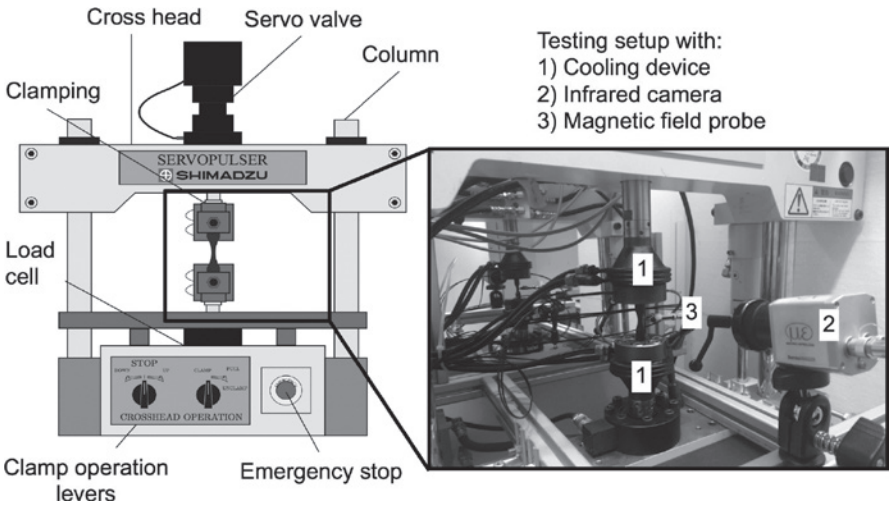

Figure 2: Experimental setup

(Wt.–%)		C	Si	Mn	P	S	Cr	Mo	Ni
DIN	min.	0.42	–	0.50	–	–	–	–	–
	max.	0.50	0.40	0.80	0.030	0.035	0.40	0.10	0.40
Customer's report		0.47	0.23	0.72	0.012	0.013	0.06	0.014	0.07

Table 1: Chemical composition of normalized SAE 1045 (C45E)

Parameters	DIN	Customer's information
Yield strength $R_{p0.2}$ (MPa)	min. 305	413
Tensile strength R_m (MPa)	min. 580	710
Ultimate strain A (%)	min. 16	23.5
Notch impact strength KCU ($J_m cm^{-2}$)	–	56
Hardness (HB)	–	210

Table 2: Mechanical and quasistatic properties of normalized SAE 1045 (C45E)

Methods and material

Material. The SAE 1045 (C45E) steel is in accordance with DIN EN 10083-1. The material was delivered in the form of round bars with a length of 5,000 mm and a diameter of 20 mm and a scaly surface due to heat treatment. The heat treatment by the manufacturer consisted of austenitization at 850 °C, followed by a controlled, slow cooling process to ambient temperature to receive a mostly ferritic-pearlitic microstructure which is shown in a light micrograph in Figure 1a.

In the micrograph, ferrite is displayed as whitish, and the pearlite is characterized by cementite lamellas (black) and ferrite (white) regions in between. The geometry of the fatigue specimen is given in Figure 1b.

The SAE 1045 (C45E) steel in the normalization condition has a Brinell hardness of 210 and a mostly ductile material behavior due to applied loads. The chemical composition from a comparison with DIN EN 10083-1 as well as the mechanical and quasistatic properties are summarized in Table 1 and 2 [9].

Experimental setup. Stress-controlled load increase (LITs) and constant amplitude tests (CATs) were carried out at ambient temperature at a frequency of 5 Hz on a servo-hydraulic testing system type EHF-L by Shimadzu with a maximum cyclic/quasistatic load of 20/25 kN using a sinusoidal load-time function at a load ratio of R = -1. The complete experimental setup is shown in Figure 2.

All fatigue tests were performed at the Chair for Non-Destructive Testing and Quality Assurance at Saarland University for a maximum number of cycles N_{max} of 2×10^6 or until specimen failure. To characterize the microstructure-based fatigue behavior in detail, the change in temperature ΔT was calculated from the surface temperature of the specimen, measured along the gauge length by an infrared camera continuously during the fatigue tests.

This quantitative change is directly related to deformation-induced changes in the microstructure in the bulk material and is considered to represent the current fatigue state. Since metallic materials are very good heat conductors, the microstructure related dissipated energy is superim-

posed by heat transfer processes, which require a temperature stabilized grip system for the servo-hydraulic test setup.

For the following temperature measurements, three fields (5 × 5 pixel) were defined along the specimen, one in the middle of the gauge length (T_1) and two at each shaft (T_2, T_3). The change in temperature was calculated in accordance to Equation (1) below:

$$\Delta T = T_1 - 0.5 \times (T_2 + T_3) \quad (1)$$

The diameter of the shafts is much larger than the diameter of the gauge length, and due to this the elastic portion of the change in temperature as well as the ambient influences are reduced from T_1, which leads to ΔT. ΔT is proportional to the plastic strain amplitude $\varepsilon_{a,p}$ and is dedicated to the plastic deformations in the specimen gauge length.

The temperature was measured at a static point and due to the load ratio of – 1, there was nearly no elongation of the specimen. The oscillation on the specimen's surface during cyclic loading was not taken into account.

Figure 3 underlines the capability of using temperature measurements to characterize the cyclic deformation behavior in a CAT with a stress amplitude of σ_a = 375 MPa in terms of the temperature based cyclic deformation curve calculated in accordance to Equation (1) and related thermographs at 5, 50 and 95 % of the lifetime.

It can be observed that the zones of plastic deformation expand continuously, and the dissipated energy increases as the fatigue progress increases. In contrast to the temperature based cyclic deformation curve, the thermographs show the absolute values of the temperature, which are not referenced to the initial image or value at the beginning of the constant amplitude test.

The theoretical background can be deduced from a consideration of the stress-strain hysteresis loop. The area of the hysteresis loop describes the energy that must be applied to plastically deform the specimen during cyclic loading. Since energy cannot simply be extinguished, it is transformed into internal energy U and heat energy Q [4]. The internal energy enables microstructural changes such as dislocation reactions, micro- and macro-cracking and their propagation. A predominant proportion of about 90 % of the deformation energy dissipates as heat, which is why temperature change can be correlated directly with plastic deformation or cumulative damage. In the case of metallic materials, the change in temperature due to dissipated heat energy can be easily measured on the specimen surface due to very good heat conduction.

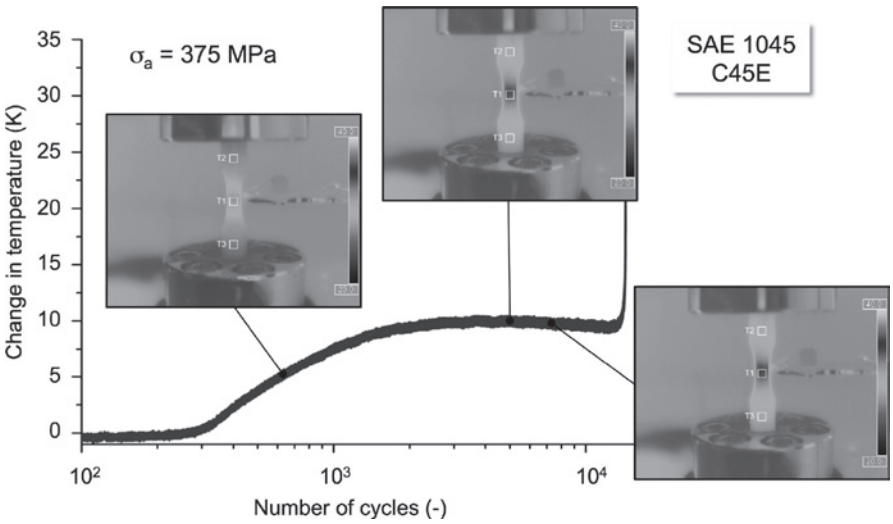

Figure 3: Cyclic deformation curve based on the change in temperature for a constant amplitude test with a stress amplitude of σ_a = 375 MPa and corresponding thermographs at 5, 50 and 95 % N_f of normalised SAE 1045

For temperature measurements, the specimen was painted black and an emission factor of 0.97 was determined. Due to the black color as well as the fact that the temperature changes are very small in the case of normalized SAE 1045 (C45E) steel, the change in emissivity can be neglected for black-colored specimens even if temperature changes are relatively small (< 10 K).

For these investigations, an infrared camera type thermoIMAGER TIM 450 by Micro-Epsilon was used. This system provides a spectral range of 7.5-13 µm, an optical resolution of 382 × 288 pixels and a thermal sensitivity of 40 mK. The data acquisition software was programmed according to the requirements of the fatigue tests on National Instruments LabView 2015. The software allows for the extraction of thermographs and ther measurement of point/line/field temperatures on the specimen's surface.

For the sake of thermal stability as well as accuracy during the long test intervals, the infrared camera was modified by an active cooling system (see Figure 2).

To maintain the thermal stability of the specimen grips, a cooling system based on Peltier-elements with water coolant was developed. This system is capable of reducing the temperature difference between the upper and lower grip during the test to less than 1 K as well as the temperature drift during the test to less than 1 K.

Theory

The StressLife$_{tc}$ approach gives comprehensive information regarding load-function related deformation behavior and thus the load-lifetime relation by means of the S-N curve of a material by using only one load increase and two constant amplitude tests. The material response is measured by NDT-related methods, in this case, for example, the change in temperature through an infrared camera.

In the following, Morrow [10], Manson-Coffin [11] and Basquin [12] laws are combined into one single equation in order to calculate the S-N data for the material investigated.

The first step in the StressLife$_{tc}$ procedure is a load increase test starting from a stress amplitude $\sigma_{a,start}$, which is chosen significantly below the fatigue limit of the investigated material (see Figure 4a). For most materials with a yield to tensile strength ratio $0.50 < R_{p0.2} \times Rm^{-1} < 0.65$ ($R_{p0.2}$: yield strength, Rm: tensile strength), this value can be set to $\sigma_{a,start} < 0.5 \times R_{p0.2}$.

Then, the stress amplitude σ_a is increased by $\Delta\sigma_a$ after each step with the step length ΔN (N: number of cycles) until specimen failure. Here, the material response is recorded and is used to characterize the cyclic deformation behavior in the LIT providing information regarding stress-material response behavior as well as a first estimation of fatigue strength based on the evaluation of the first micro-plastic deformations. Moreover, it is possible to identify appropriate stress amplitudes for the two CATs, which both have to be performed in the elastic-plastic range which can be derived from the LIT (see Figure 4c).

From the traditional point of view, the material response for stress-controlled tests is the total and plastic strain amplitude, but this can also be transferred to

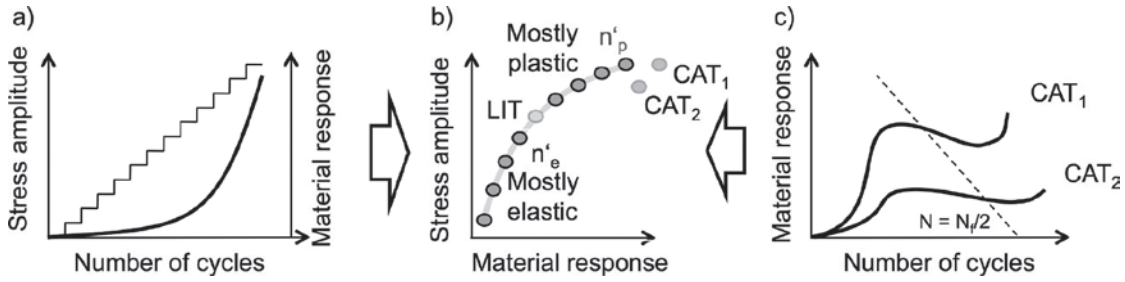

Figure 4: a) Load increase test, b) generalized Morrow diagram, c) cyclic deformation curves of the two constant amplitude tests in accordance to the StressLife$_{tc}$ method, schematically

other measuring methods like the change in temperature or any changes in magnetic or electric parameters and due to this can be written in a generalized manner [8-9].

For further calculation, the stress amplitude is plotted vs. the material response in terms of a generalized Morrow plot [9-10], which is shown in Figure 4b.

From this diagram, a mostly elastic and a mostly plastic range can be identified and described independently of each other mathematically according to Morrow expressed through Equation (2).

$$\sigma_a = K_{e/p/CAT'} \cdot (M)^{n_{e/p/CAT'}} \quad (2)$$

From Equation (2) and the differentiation into a mostly elastic and mostly plastic range (see Figure 4b), the fatigue strength exponent b (mostly elastic range) as well as the fatigue ductility exponent c (mostly plastic range) can be calculated by using Equations (3) and (4).

$$b = \frac{-n_e'}{5n_e'+1} \quad (3)$$

$$c = \frac{-1}{5n_p'+1} \quad (4)$$

As previously explained for the term "material response", the measured value M can be, for example, the plastic strain amplitude, the change in temperature, the change in electrical resistance or the change in the magnetic parameter, and can be specified into an elastic (M_e) and a plastic (M_p) portion in Equation (5).

$$M_t = M_e + M_p \quad (5)$$

M_e can be represented by a generalized Basquin equation (Equation (6)), where, in the case of strain measurements, B is expressed by $\sigma_f' \times E^{-1}$ (σ_f' = fatigue strength coefficient, E = Young's modulus).

$$M_e = B \cdot (2N_f)^b \quad (6)$$

M_p can be described by Manson-Coffin (Equation (7)), where C corresponds to the fatigue ductility coefficient ε_f', if strain is the measured value.

$$M_p = C \cdot (2N_f)^c \quad (7)$$

If Equation (7) and (6) are used in Equation (5), then Equation (8) is obtained:

$$M_{1/2} = B \cdot (2N_{f,1/2})^b + C \cdot (2N_{f,1/2})^c \quad (8)$$

As has already been shown in Figure 4c, two CATs ($\sigma_{a,2} < \sigma_{a,1}$) are performed leading to different number of cycles to failure ($N_{f,2} > N_{f,1}$) as well as to different values of the material response ($M_2 < M_1$) at a defined fatigue stage, e. g. $0.5 \times N_f$.

$$C = \frac{(2N_{f,1})^b \cdot M_2 - (2N_{f,2})^b \cdot M_1}{(2N_{f,2})^c \cdot (2N_{f,1})^b - (2N_{f,1})^c \cdot (2N_{f,2})^b} \quad (9)$$

Since there are two values each for N_f and M, C (Equation (9)) and B (Equation (10)) can be evaluated through this.

$$B = \frac{M_1 - C \cdot (2N_{f,1})^c}{(2N_{f,1})^b} \quad (10)$$

In consequence of Equations (6) and (7), the elastic as well as plastic portion of the material response can be plotted vs. the number of cycles to failure, which is shown in Figure 5a as slopes indicated with b and c. The summation of both curves leads to a material response-number of cycles to failure- (MR-N-) curve. According to the simplification of Ramberg-Osgood [13], the elastic behavior can be assumed to be linear. By extrapolation of the elastic portions of M_1 (CAT_1) and M_2 (CAT_2) to a σ_a-value ($CAT_{calc.}$) slightly above the transition point from a mostly elastic to mixed elastic-plastic behavior, M_e for σ_a of $CAT_{calc.}$ can be calculated. By using the relationship between M_e (slope b) and the MR-N-curve, M_t can be calculated for $CAT_{calc.}$ (see Figure 5b). With this third calculated point, K_{CAT}' and n_{CAT}' can now be determined according to Equation (2).

If Equation (8) is used in Equation (2), then Equation (11) follows, the parameters C, B, K_{CAT}' and n_{CAT}' being determined in the preceding steps. Based on Equation (11), the S-N curve can be calculated (Figure 5c).

$$\sigma_a = K_{CAT}' \cdot (B \cdot (2N_f)^b + C \cdot (2N_f)^c)^{n_{CAT}'} \quad (11)$$

Results

Load increase tests (LIT) allow for estimating the fatigue limit of materials with only one specimen. In Figure 6, beside the stress amplitude σ_a, starting at $\sigma_{a,\,start}$ = 200 MPa with a stepwise increase of $\Delta\sigma_a$ = 20 MPa each $\Delta N = 6 \times 10^3$ cycles, the change in temperature ΔT is plotted versus the number of cycles for a specimen of normalized SAE 1045 (C45E) steel. The change in temperature is calculated according to Equation (1) and is shown in Figure 6 together with the stress amplitude in the range of 30×10^3 number of cycles until failure. From $N = 36 \times 10^3$ and σ_a = 320 MPa and upwards, there is a slight change in the ΔT-slope indicating the first micro-plastic deformations. Based on this result, the fatigue limit (point of transition) can be estimated as having a value of σ_a = 300 MPa and this value agrees very well with the transition to the fatigue strength of normalized SAE 1045. It is impressive that from this single test, the fatigue limit can be estimated in very good accordance with the conventionally determined fatigue limit, which is expressed in Figure 11.

By using the ΔT-values of each load level from the middle of the step from the LIT (see Figure 6), a cyclic stress amplitude-change in temperature- (CST-) curve can be generated, which is plotted in Figure 7. As mentioned before, from these values a mostly elastic and a mostly plastic range can be identified. In order to prevent any mixing of these two areas, the data points directly before and after the point of transition (σ_a = 300 MPa) are not included in the further calculation. These 3 points are displayed in the diagram as single rhombs without straight lines. The mathematical description of the two ranges is given according to Equation (2). Based on the val-

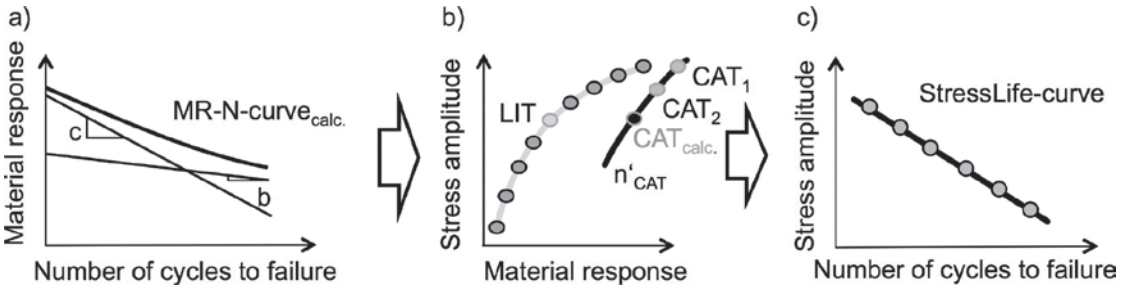

Figure 5: a) Material response-number of cycles-curve, b) generalized Morrow diagram and c) S-N-curve calculated in accordance to the StressLife$_{tc}$ method, schematically

ues of n_e' and n_p', b and c can be calculated through Equation (3) and Equation (4).

In addition to the LIT, two CATS were performed. The stress amplitudes for both CATs were chosen above the point of transition. The frequency was kept constant during the CATs, which possibly leads to an influence in the mechanical stress rate, which was not considered separately in the following. The mechanical stress rate is reduced by less than 25 % from the CAT with σ_a = 380 MPa to the CAT with σ_a = 320 MPa, so the influence here should be negligible.

Thus, Figure 8 shows cyclic deformation curves with stress amplitudes of σ_a = 320 MPa and 380 MPa in terms of the change in temperature vs. the number of cycles N.

The cyclic deformation behavior is characterized by varying incubation intervals with ΔT values close to zero until first cyclic softening at increasing ΔT values. For the CAT with σ_a = 380 MPa, after passing the cyclic softening maximum, cyclic hardening leads to decreasing ΔT-values until just before failure. In the case of the CAT with σ_a = 320 MPa, after a first cyclic softening a saturation state follows. The macroscopic crack formation and propagation leads to fictive secondary cyclic softening.

Following Equations (6) to (11) by using the σ_aT-values at 0.5 × N_f (see Figure 8: marked with symbols) as well as N_f of the two CATs, B and C can be calculated. Based on the calculated parameters of the fatigue strength coefficient B, the fatigue ductility coefficient C, the fatigue strength exponent b and the fatigue ductility exponent c, Equation (8) leads to the change in temperature-number of cycles to failure- (ΔT-N-) curve in Figure 9. This relationship describes not the individual cyclic deformation behavior of a single specimen as given in Figure 8. It rather shows how the general relationship between σ_a and ΔT at 0.5 × N_f cycles can be described.

In accordance to Ramberg-Osgood, the elastic portion of the material response can be assumed as linear from which the elastic part of the ΔT-value of a CAT σ_a = 300 MPa can be calculated. If the relationship between the elastic and plastic portion vs. the number of cycles to failure from Figure 9 is used, ΔT can be calculated for a CAT with σ_a = 300 MPa.

If this calculated ΔT-value as well as the conventional determined ones from the

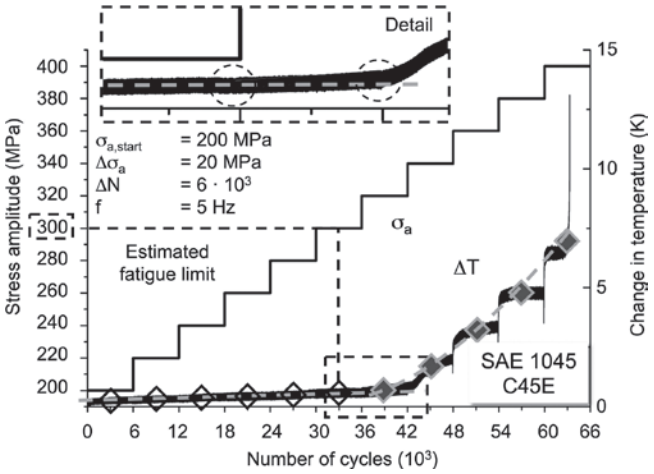

Figure 6: Load increase test with the courses of the stress amplitude and the change in temperature of normalized SAE 1045

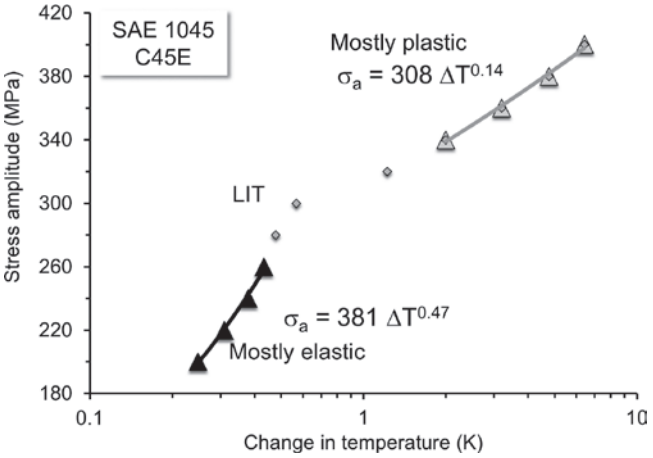

Figure 7: Stress amplitude-change in temperature-relation of the load increase test shown in Figure 6 with identified ranges of mostly elastic and mostly plastic cyclic deformation behavior of normalized SAE 1045

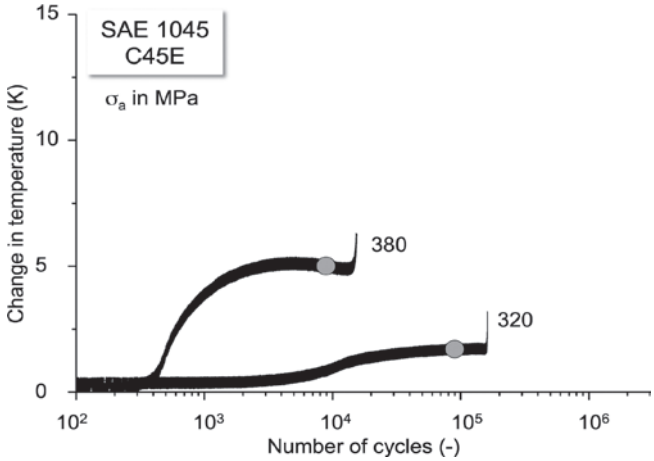

Figure 8: Temperature based cyclic deformation curves for two constant amplitude tests with stress amplitudes of σ_a = 320 MPa and 380 MPa of normalized SAE 1045

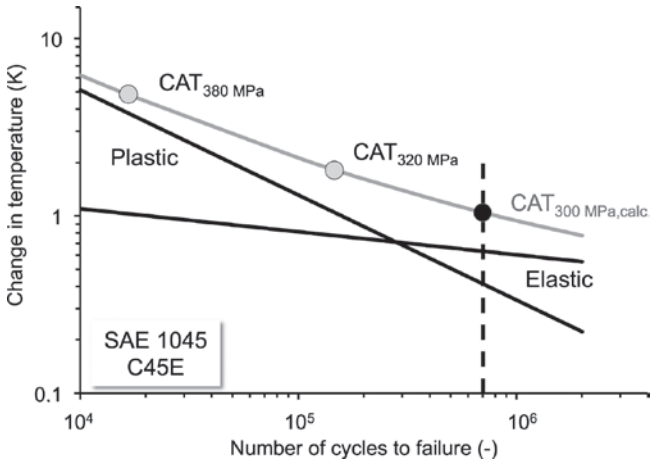

Figure 9: Change in temperature-number of cycles to failure-curve based on Equation (8) and the calculated parameters of b, c and B, C of normalized SAE 1045

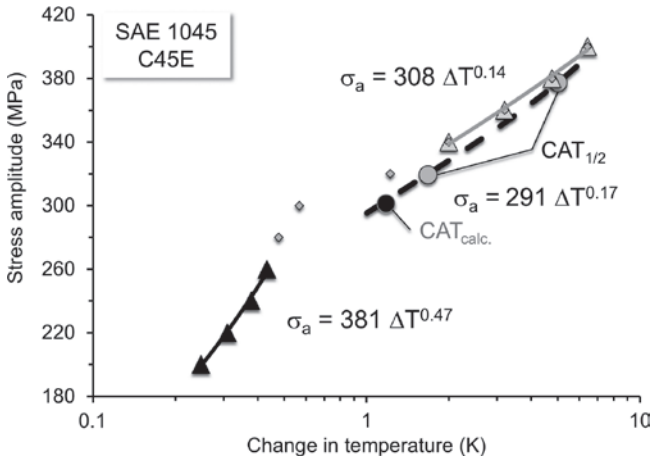

Figure 10: Stress amplitude-change in temperature-relation of the load increase test and the constant amplitude test of normalized SAE 1045

two CATs are plotted together at the appropriate stress amplitude, the CST-curve for CATs can be evaluated. From the mathematical description (Equation (2)), K' as well as n' can be determined (see Figure 10). By using the coefficients B, C and K' as well as the exponents b, c, and n' in Equation (12), an S-N curve can be calculated, which is presented in Figure 11.

Figure 11 gives an impression regarding the capability of the $StressLife_{tc}$ approach, which enables the calculation of a material's fatigue life based on one load increase and two constant amplitude tests and is in very good accordance compared to the conventional determined lifetimes from constant amplitude tests. This result underlines that the $StressLife_{tc}$ approach could lead to an enormous reduction in time and cost, while the experimental efforts might also be reduced, so that significant financial as well as scientific advantages may be reached.

Discussion

In Figures 3 and 6, it can be seen, that temperature measurements are very well suited to characterize the cyclic deformation behavior of metallic materials in load increase and constant amplitude tests. The mechanical energy responsible for the plastic deformation of the specimen during cyclic loading dissipates in heat energy by approx. 90 %, whereas the residual 10 % results in microstructural change as dislocation reactions, micro- and macro-crack formation and propagation etc. Due to this, temperature measurements offer the possibility of giving information very locally. Moreover, small plastic deformations can be measured even better than in the case of conventional mechanical stress-strain-hysteresis measurements, which supply more integral information along the whole gauge length of the extensometer. This can be compared in terms of point (temperature) and line (strain) information. Moreover, in the case of temperature measurements, no cylindrical gauge length is needed, which also makes it possible to use this technique in the case of notched specimens or even components and complex structures.

These significant advantages are not limited to temperature measurements only but can be transferred, for example, to magnetic and electrical measurement methods. Figure 12 shows the same load increase test as in Figure 6 but in this case with the course of the stress amplitude and the material response in terms of the electrical voltage signal of a fluxgate sensor which measures the change in magnetic field strength perpendicular to the sample axis without further magnetization. It can be seen that during mostly elastic loading the signal increases more or less linearly to the increase in stress amplitude which can be explained by the elastic distortion of the lattice structure. The magnetic sensor thus reflects the deformation of the lattice. At σ_a = 280 MPa, this behavior changes and the fluxgate signal reaches a local maximum of σ_a = 300 MPa which correlates with the fatigue limit estimated in LIT and evaluated in the CATs. The current explanation suggests that the increase in dislocation density in the range of first micro-plastic deformations reduces the distortions of the crystal lattice, causing the magnetic signal to stagnate and even to fall off for a further increase in the stress amplitude. Independently of this, Figure 12 shows that NDT-based measurement methods are very well-suited to display even small changes in the material microstructure.

Based on these measuring methods valuable parameters for fatigue life calculation can be provided. The StressLife method as one of them makes it possible to calculate S-N curves on the basis of results of just three fatigue tests. However, it must be noted that material behavior can sometimes scatter strongly. In many cases, this depends on the material itself, but may also be due to the material condition. For this reason, the results calculated according to StressLife must always be considered critically. In ad-

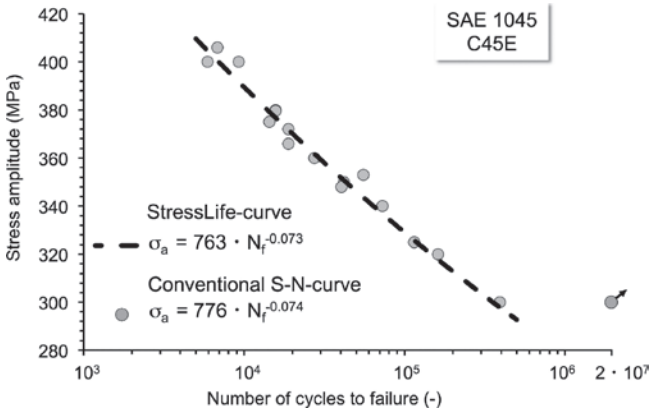

Figure 11: Comparison of conventional determined fatigue data with the calculated $StressLife_{tc}$-curve of normalized SAE 1045

dition, this method supplies a wealth of information regarding cyclic deformation behavior which makes it a valuable tool for material characterization under cyclic loading. For example, it might be possible to compare results of stress- and strain-controlled fatigue tests with one another and even to convert them for a first estimation. Therefore, the separation of a total deformation into elastic and plastic portions (see Figure 9) as known from S-N curves evaluated under total strain control is a basic requirement. This procedure must be further examined and validated in follow-up investigations which include not only additional fatigue tests but more analytical investigations.

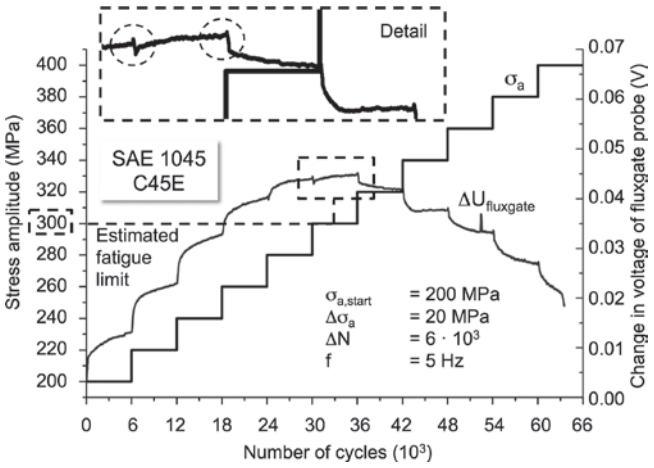

Figure 12: Load increase test with the courses of the stress amplitude and the change in voltage of a fluxgate sensor of normalized SAE 1045

Conclusions

In addition to extensometers and strain gauges, additional measurement techniques have been introduced in the last decades. Recently, NDT-methods based on thermal and magnetic sensing technologies have drawn increasing attention to the determination of fatigue relevant parameters. As these approaches are closely associated with the physical features of materials, they might be of benefit for short-term procedures or fatigue life calculation methods.

The above-mentioned measuring techniques are highly sensitive to initial microstructural changes due to dislocation reactions and could therefore offer significant advantages in comparison with conventional methods based on stress or strain measurements. Furthermore, material properties determined by these techniques are independent of a defined gauge length and also applicable to complex geometries like notched specimens or even components.

Within the new fatigue life calculation method, StressLife$_{tc}$ fatigue data from one load increase and two constant amplitude tests were used in order to evaluate the fatigue strength as well as the fatigue limit of a metallic material. This short-time procedure allows for a reduction in efforts through experimentation by more than 90 % and therefore offers a possibility for focusing on more fatigue relevant parameters, which improve the S-N curve to a multidimensional dataset.

Acknowledgements

The author would like to thank the German Research Foundation (Deutsche Forschungsgemeinschaft DFG) for financial support for this research (STA 1133/6-1). The author would also like to thank Shimadzu Europe and Micro-Epsilon for their support in providing technical equipment.

References

1 P. Lukáš, M. Klesnil: Cyclic stress-strain response and fatigue life of metals in low amplitude region, Materials Science and Engineering 11 (1973), pp. 345-356 DOI: 10.1016/0025-5416(73)90125-0
2 A. Brazenas, D. Vaiciulis: Determination of fatigue curve parameters at cyclic strain limited loading according to the mechanical characteristics of power energy structural materials, Nuclear Engineering and Design 241 (2011), pp. 3596-3604 DOI: 10.1016/j.nucengdes.2011.07.022
3 F. Curà, A. E. Gallinatti, R. Sesana: Dissipative aspects in thermographic methods, Fatigue & Fracture of Engineering Materials and Structures 35 (2012) No. 12, pp. 1133-1147 DOI:10.1111/j.1460-2695.2012.01701.x
4 G. Meneghetti, R. B. Atzori: A two-parameter, heat energy-based approach to analyze the mean stress influence on axial fatigue behavior of plain steel specimens, International Journal of Fatigue (2016), pp. 60-70 DOI:10.1016/j.ijfatigue.2015.07.028
5 G. Dobmann, A. Seibold: First attempts towards the early detection of fatigued substructures using cyclic-loaded 20MnMoNi5 5 Steel, Nuclear Engineering and Design 137 (1992), pp. 363-369 DOI:10.1016/0029-5493(92)90259-X
6 H. Huang, S. Jiang, R. Liu, Z. Liu: Investigation of Magnetic Memory Signals Induced by Dynamic Bending Load in Fatigue Crack Propagation Process of Structural Steel, Journal of Nondestructive Evaluation 33 (2014), pp. 407-412 DOI:10.1007/s10921-014-0235-y
7 M. A. Miner: Cumulative damage in fatigue, Journal of Applied Mechanics 12 (1945), pp. 159-164
8 P. Starke, F. Walther, D. Eifler: "PHYBAL" a short-time procedure for a reliable fatigue life calculation, Advanced Engineering Materials 12 (2010), No. 4, pp. 276-282 DOI: 10.1002/200900344
9 P. Starke, H. Wu, C. Boller: Advanced Evaluation of Fatigue Phenomena Using Non-Destructive Testing Methods, Material Science Forum, 879 (2016), pp. 1841-1846 DOI:10.4028/879.1841
10 J. D. Morrow: Cyclic plastic strain energy and fatigue of metals. Internal friction, damping and cyclic plasticity, American Society for Testing and Materials (1964), pp. 45-87
11 M. Ricotta: Simple expressions to estimate the Manson–Coffin curves of ductile cast irons, International Journal of Fatigue 78 (2015), pp. 38-45 DOI:10.1016/j.ijfatigue.2015.03.025
12 O. H. Basquin: The exponential law on endurance tests, American Society for Testing and Materials 10 (1910), pp. 625-630
13 J. Li, Z. Zhang, C. Li: An improved method for estimation of Ramberg–Osgood curves of steels from monotonic tensile properties, Fatigue & Fracture of engineering materials & structures 39 (2016), pp. 412-426 DOI:10.1111/ffe.12366

Bibliography

DOI 10.3139/120.111319
Materials Testing
61 (2019) 4, pages 297-303

ISSN 0025-5300

The author of this contribution

Prof. Dr.-Ing. Peter Starke, born in 1977, studied Mechanical Engineering at the TU Kaiserslautern, Germany. Since 2002, he has been a research assistant at the Institute of Materials Science and Engineering (WKK) at TU Kaiserslautern, Germany. He received his Doctorate in Engineering in 2007 writing on "The fatigue life calculation of metallic materials under constant amplitude loading and service loading". From 2007 to 2012, he headed the research group "Fatigue life calculation" at the WKK. Afterwards, he took a position at the Fraunhofer IZFP in Saarbrücken, Germany. From 2013 to 2018 he was a Senior Research Associate at the Chair of Non-Destructive Testing and Quality Assurance at Saarland University in Saarbrücken, Germany. 2018 he became a Professor in the field of Materials Science and Materials Testing at the University of Applied Sciences Kaiserslautern (Hochschule Kaiserslautern), Germany. His research mainly focuses on the use of nondestructive measurement techniques for the characterization of fatigue behavior and the fatigue life calculation of metallic and non-metallic materials in the realm of LCF-, HCF- and VHCF as well as for the evaluation of defects and inhomogeneities in materials microstructure.